ENVIRONMENTAL RESEARCH
LETTERS

LETTER • OPEN ACCESS

How likely is an El Niño to break the global mean surface temperature record during the 21st century?

To cite this article: Chia-Wei Hsu and Jianjun Yin 2019 *Environ. Res. Lett.* **14** 094017

View the article online for updates and enhancements.

You may also like

- The role of external forcing and internal variability in regulating global mean surface temperatures on decadal timescales
Lu Dong and Michael J McPhaden
- The contribution of greenhouse gases to the recent slowdown in global-mean temperature trends
R Checa-Garcia, K P Shine and M I Hegglin
- Structure Effects for 3417 Celestial Reference Frame Radio Sources
M. H. Xu, J. M. Anderson, R. Heinkelmann et al.

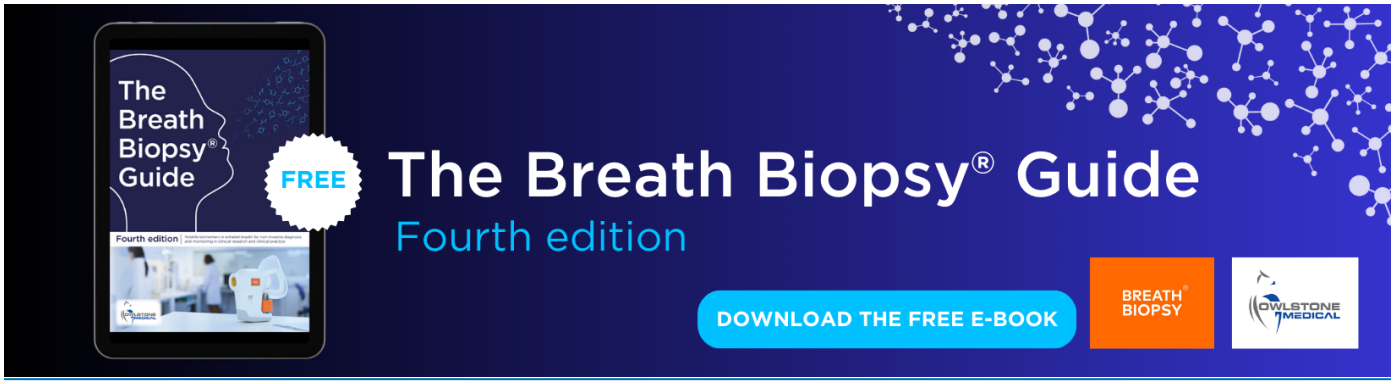

This content was downloaded from IP address 137.75.80.24 on 11/01/2024 at 18:02

Environmental Research Letters

LETTER

How likely is an El Niño to break the global mean surface temperature record during the 21st century?

Chia-Wei Hsu and Jianjun Yin

University of Arizona, Department of Geoscience, 1040 E 4th St, Tucson, AZ 85721, United States of America

E-mail: chiaweih@email.arizona.edu

Keywords: CMIP5, global mean surface temperature, El Niño, record-breaking

Supplementary material for this article is available online

OPEN ACCESS

RECEIVED
2 May 2019

REVISED
8 August 2019

ACCEPTED FOR PUBLICATION
15 August 2019

PUBLISHED
13 September 2019

Original content from this work may be used under the terms of the Creative Commons Attribution 3.0 licence.

Any further distribution of this work must maintain attribution to the author(s) and the title of the work, journal citation and DOI.

Abstract

The likelihood of an El Niño breaking the annual global mean surface temperature (GMST) record during the 21st century is derived from 38 climate models from the Fifth Coupled Model Intercomparison Project (CMIP5). We find that, under a low emission scenario, one out of three El Niño events break the GMST record. The probability significantly increases to four out of five in a high emission scenario. About half of strong El Niños, but only one-fifth of weak El Niños, can set new GMST records in a low emission scenario. By contrast, even weak El Niños break the GMST record more regularly (68 ± 8% chance) in a high emission scenario. Both a stronger El Niño and a higher emission scenario induce a higher record-breaking GMST with a magnitude range from 0.03°C to 0.21°C above the previous record. El Niño accounts for more than half of record-breaking GMST occurrences in all emission scenarios. A comparison between CMIP3, CMIP5, and CMIP6 suggests that the analyses are not affected by model generations.

1. Introduction

The efficiency and rapidity of El Niño in pushing up the record warm global mean surface temperature (GMST) have been demonstrated in recent decades, notably during the strong 1997/98 and 2015/16 El Niños. As a naturally-occurring phenomenon, an El Niño can cause a strong and transient warmth of the global climate, superimposed on the gradual and persistent warming induced by greenhouse gas (GHG) forcing (Newell and Weare 1976, Pan and Oort 1983, Timmermann *et al* 1999, Trenberth 2002). The gradual background warming continues to shift the probability distribution of GMST toward higher values, thereby increasing the chance of record-breaking GMST once any internal fluctuation occurs (Wergen and Krug 2010). Recently, Power and Delage (2019) demonstrate the likelihood of a monthly record-breaking surface temperature occuring under different future scenarios. Since 1980, 11 out of 14 record-breaking annual GMSTs have coincided with an El Niño event (Yin *et al* 2018). Over a long period, these record-breaking GMSTs reflect the general warming trend (Su *et al* 2017), while on short timescales, they reveal extreme events with non-linearity or threshold behaviors inherent in the climate system (Yin *et al* 2018).

The interactions between El Niño and global warming and their combined effect on GMST are important topics in climate change detection and attribution (Foster and Rahmstorf 2011). During the 21st century, GHG forcing is projected to alter the characteristics and statistics of El Niño, such as its frequency, amplitude, duration, pattern, and teleconnection (Chen *et al* 2016). Besides El Niño, other factors can also influence GMST variations on various timescales, including the Pacific Decadal Variability (PDV)/Inter-decadal Pacific Oscillation (IPO) (Meehl *et al* 2016, Su *et al* 2017), Atlantic Multi-decadal Variability (AMV) (Schlesinger and Ramankutty 1994, Zhang *et al* 2007, Muller *et al* 2013), Atlantic Meridional Overturning Circulation (Schleussner *et al* 2014), and Arctic Oscillation (AO) (Buermann *et al* 2003, Zanchettin *et al* 2013).

Regardless of the many factors listed above, Trenberth (2002) shows the importance of diabatic heating

© 2019 The Author(s). Published by IOP Publishing Ltd

from the tropical Pacific ocean on the GMST. Thus, when an El Niño occurs during the 21st century, an important question for near-term climate change prediction would be: *how likely is the El Niño to break the GMST record, and by how much*? To answer this, we analyze the historical simulations and future projections from 38 climate models in the Fifth Coupled Model Intercomparison Project (CMIP5) (Taylor *et al* 2011), supplemented with the results from CMIP3 and CMIP6. It should be noted that we do not attempt to make actual and real-time predictions for particular events, but rather to obtain the statistics from the CMIP5 models about El Niño, global warming, and record-breaking GMST. We evaluate these statistics for each model before calculating their multi-model ensemble mean.

2. Models and methods

The CMIP5 multi-model ensemble has demonstrated improvements on the convergence of El Niño amplitude and life cycle between models when compared to CMIP3 (Bellenger *et al* 2014). To identify the El Niño events and associated record-breaking GMSTs during the 21st century (2006–2100), we use the monthly 'tos' and 'tas' outputs from a total of 38 CMIP5 models under the same ensemble run and calculate the Oceanic Niño Index (ONI) and GMST. The variable 'tos' and 'tas' represent sea surface temperature (SST) in the oceanic models and the near-surface (two-meter) air temperature in the atmospheric models, respectively. The ONI is routinely used by the Climate Prediction Center (CPC) at the National Oceanic and Atmospheric Administration (NOAA) to monitor the condition of the tropical Pacific and to issue El Niño/La Niña warnings once thresholds are passed (https://origin.cpc.ncep.noaa.gov/products/analysis_monitoring/ensostuff/ONI_v5.php).

To obtain the ONI in the CMIP5 models, we calculate the area-weighted mean of monthly SST anomalies in the Niño 3.4 region (5°N–5°S, 170°W–120°W) with the seasonal climatology and long-term trend removed before calculating the three-month running mean. The detrending follows the method from the CPC by removing the 30-year means from every five years centered at the 30-year window. This avoids the trend affecting the identification of the El Niño events in different Representative Concentration Pathways (RCP) scenarios. An El Niño event is identified whenever the ONI is higher than 0.5 °C for more than five consecutive months, the same criteria set by the CPC. We also tested two other methods for ONI detrending, including the removal of either the linear trend or low-frequency component identified with a low-pass Butterworth filter. All three methods generate results with variations within the error bar shown in this study. In this study, we use the CPC method to determine El Niño.

For the GMST in each model and RCP, we first derive a monthly time series of GMST from the area-weighted average of 'tas' with the seasonal cycle removed. We further calculate an annual mean time series to identify the record-breaking annual GMSTs. For each model, we set 1850–1899 in the historical run as the reference period to identify the first record-breaking GMST and then the following records during the 20th and 21st centuries.

Trenberth (2002) has shown that the GMST response typically lags the Niño 3.4 index by around three months in the observational data. Therefore, we pick out the years where the record-breaking annual GMST is overlapped by the period that is a three-month lag to an El Niño period (figure 1(a)). However, there is a possibility that one could make an incorrect linkage between El Niño and record-breaking GMST. This happens when record-breaking GMSTs are largely induced by other mechanisms, and coincide with the year of El Niño onset. To avoid any incorrect attribution to El Niño, we consider two particular situations based on the onset time of El Niño (figure 1(b)). In the case of the onset happening in the first half of year 1, we calculate the mean of the monthly GMST with the seasonal cycle removed after the El Niño onset. If it is higher than the annual mean GMST, only then do we attribute the record-breaking GMST to the occurrence of the El Niño. In the case of the El Niño onset happening in the second half of year 1, we do not associate the GMST, if record-breaking, with this El Niño. This is because the El Niño does not have enough time to significantly influence the annual mean GMST given the three-month lag.

We calculate the likelihood (%) of an El Niño to break the GMST record according to

$$P(\widehat{T}|\epsilon) = \frac{N_\epsilon(\widehat{T} \cap \epsilon)}{N_\epsilon} \times 100, \quad (1)$$

where $\widehat{T}$ and ϵ represent a record-breaking GMST and El Niño event, respectively. N_ϵ is the total number of El Niño events. $N_\epsilon(\widehat{T} \cap \epsilon)$ is the number of El Niños that induce at least one record-breaking GMST. In other words, $P(\widehat{T}|\epsilon)$ represents, in all El Niño events, the probability of an El Niño to induce record-breaking GMST. Similarly, we calculate the fraction of record-breaking GMST years attributable to the occurrence of an El Niño according to

$$P(\epsilon|\widehat{T}) = \frac{N_{\widehat{T}}(\widehat{T} \cap \epsilon)}{N_{\widehat{T}}} \times 100, \quad (2)$$

where $N_{\widehat{T}}$ is the total number of record-breaking GMSTs. $N_{\widehat{T}}(\widehat{T} \cap \epsilon)$ is the number of record-breaking GMSTs induced by El Niño. Figure 1(c) shows the relation between the different numbers used in the equations above ($N_{\widehat{T}}$, N_ϵ, $N_{\widehat{T}}(\widehat{T} \cap \epsilon)$, $N_\epsilon(\widehat{T} \cap \epsilon)$). The number of record-breaking GMSTs that are induced by an El Niño ($N_{\widehat{T}}(\widehat{T} \cap \epsilon)$) can differ from the number of El Niños that induce at least one record-breaking GMST ($N_\epsilon(\widehat{T} \cap \epsilon)$) due to occasional

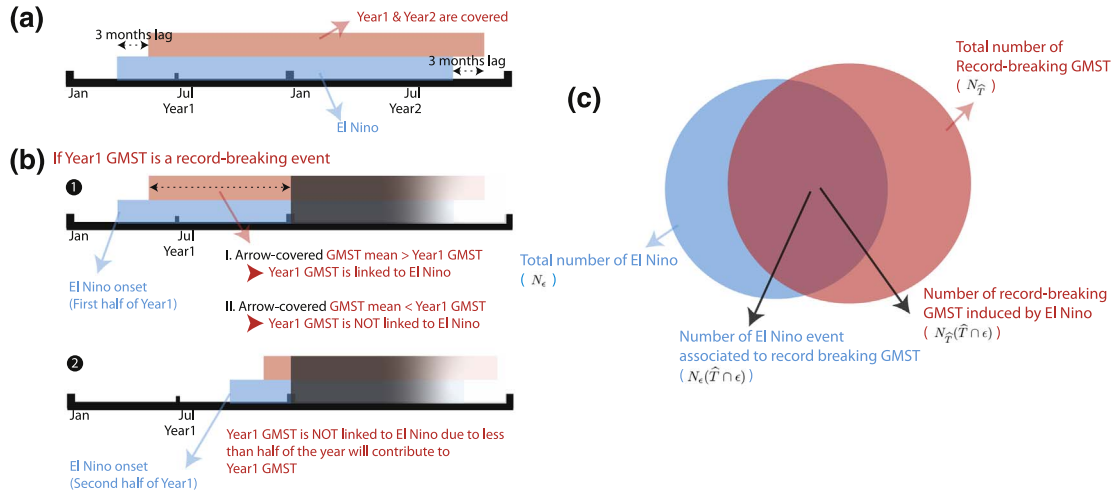

Figure 1. The schematic diagram describes the methods used in this study to pick the record-breaking annual GMST associated with El Niño. (a) The red covered period indicates the period analyzed for record-breaking annual GMST (year 1 and year 2). If any annual GMST is a record-breaking year, it is linked to the El Niño event shown in the blue covered period except for some cases shown in (b). (b) Same as (a) for color arrangement assuming that year 1 is a record-breaking GMST while the El Niño onset happens in year 1; two cases marked by the white numbers 1 and 2 represent the El Niño onset in the first and second half of year 1, respectively. For case 1, the year 1 record-breaking GMST is linked to the El Niño event only when the arrow-covered GMST monthly mean is larger than the year 1 annual GMST. For case 2, the year 1 GMST, if record-breaking, is not attributed to the El Niño. (c) The Venn diagram shows the logical relations between the total number of El Niños (blue circle), the total number of record-breaking GMSTs (red circle), the number of record-breaking GMSTs induced by El Niño (overlapping region of red and blue circles), and the number of El Niños linked to record-breaking GMST (overlapping region of red and blue circles).

consecutive record-breaking annual GMSTs associated with one El Niño event, such as those of 2015 and 2016, associated with the 2015/16 El Niño event (Yin *et al* 2018).

We also calculate the magnitude of a record-breaking event associated with El Niño ($M(\widehat{T}|\epsilon)$). The magnitude of a record-breaking GMST is simply the difference between the new and previous records. Since there are some cases of consecutive record-breaking years associated with one El Niño event, we accumulate the record-breaking magnitudes to study the total effect of the El Niño.

We use four emission scenarios including RCP2.6, RCP4.5, RCP6.0, and RCP8.5 to study how different emission scenarios change the likelihood and magnitude during the 21st century. For any two estimated values of $X \pm x$ and $Y \pm y$, the difference is $D = |X - Y|$. The error for D is $d = \sqrt{x^2 + y^2}$ based on error propagation. D is statistically significant when $D > d$.

3. Results and discussion

3.1. Likelihood of record-breaking GMST during El Niño

To calculate the likelihood of record-breaking GMST during an El Niño ($P(\widehat{T}|\epsilon)$), we first identify El Niños, record-breaking GMSTs, and record-breaking GMSTs associated with El Niño in each model and RCP (figure 2 and figures S1–S4 available in the online supplementary material at stacks.iop.org/ERL/14/094017/mmedia). The ensemble mean of N_ϵ is 22 ± 3 in RCP2.6, 24 ± 2 in RCP4.5, 24 ± 3 in RCP6.0, and 25 ± 2 in RCP8.5 (figure 3(a)), which are consistent with the pre-industrial control (piControl) run during a 100 year period with $N_\epsilon = 23 \pm 2$. The range shown in this study represents the 95% confidence interval. The result indicates that, in most models, GHG forcing does not impact much on El Niño frequency during the 21st century. The differences in N_ϵ are relatively small between RCPs for each model (i.e., scenario uncertainty). The largest difference in N_ϵ comes from the difference between models. The multi-model ensemble mean helps reduce this structural uncertainty (Palmer *et al* 2005, Tebaldi and Knutti 2007). Most models simulate 14–35 El Niño events in their RCP projections, consistent with the El Niño cycle of 2–7 years. One model (INM-CM4) shows a significant reduction of the total number of El Niños from 28 in the historical run to 6 in the RCP projections. Internal variability and external forcing could be the possible causes for this reduction (Wittenberg *et al* 2014). By removing the three models that simulate less than 14 El Niño events in RCPs, the statistics shown in this study change by less than 5% and are still within the error bars of the ensemble mean estimates (table 1).

The number of El Niño events that are associated with record-breaking GMSTs ($N_\epsilon(\widehat{T} \cap \epsilon)$), however, increases significantly with the increasing emissions. The ensemble mean of $N_\epsilon(\widehat{T} \cap \epsilon)$ shows 8 ± 1 in RCP2.6, 13 ± 1 in RCP4.5, 14 ± 2 in RCP6.0, and 20 ± 2 in RCP8.5 (figure 3a). The differences in $N_\epsilon(\widehat{T} \cap \epsilon)$ are statistically significant between RCPs except between RCP4.5 and RCP6.0. Due to the different responses of N_ϵ and $N_\epsilon(\widehat{T} \cap \epsilon)$ to RCP changes, $P(\widehat{T}|\epsilon)$ generally follows $N_\epsilon(\widehat{T} \cap \epsilon)$, which increases

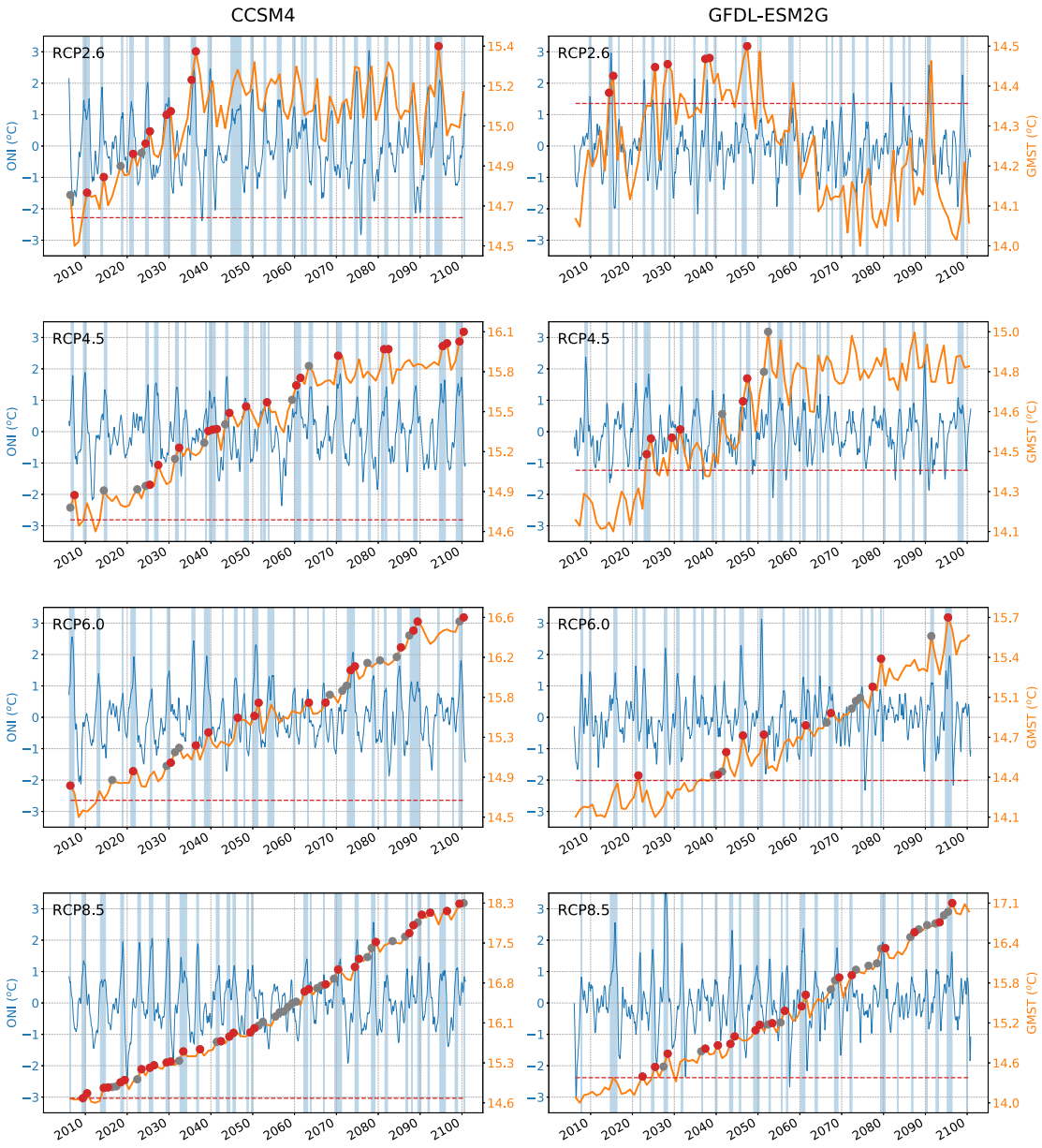

Figure 2. Identification of El Niño events and record-breaking GMSTs in two CMIP5 models—CCSM4 (left panel) and GFDL-ESM2G (right panel). Corresponding RCP scenarios are shown on the top left corner of each plot. Each plot shows annual GMST values with the orange line (notice the GMST scales are different and on the right of each plot) and ONI values with the blue line, with the blue shaded regions indicating the identified El Niño periods. The red dots are the record-breaking GMSTs associated with an El Niño event and the gray dots are those not associated with any El Niño event. The red dotted line shows the record-breaking GMST value before 2006.

with the increasing emissions in the RCPs (table 1). Except for the insignificant difference between RCP4.5 and RCP6.0, there are significant differences between any other two scenarios. The largest increase of $43 \pm 6\%$ in $P(\widehat{T}|\epsilon)$ occurs when the emission increases from RCP2.6 to RCP8.5. The result is consistent with the fact that the larger the warming trend in GMST, the higher the chance for an internal variability to break the GMST record.

For consistency and to further investigate how different El Niño strength influences record-breaking GMST, we categorize El Niño events based on the maximum value of the three-month mean ONI during each El Niño period. El Niños are categorized into weak, moderate, and strong events with the ONI range of $0.5 < \text{ONI} \leqslant 1.0$, $1.0 < \text{ONI} \leqslant 1.5$, and $\text{ONI} > 1.5$, respectively (Trenberth 2018). Table 1 shows the ensemble mean of $P(\widehat{T}|\epsilon)$ under different categories of El Niño and RCPs (figures S6–S8). Such as with the case of all El Niño, there is a positive correlation between emission strength and $P(\widehat{T}|\epsilon)$ in each category. The larger error bars in each category are due to fewer El Niño events when compared to the all El Niño case (figures S5–S8). Despite the changes in error bar, in each category, the $P(\widehat{T}|\epsilon)$ in RCP8.5 is still significantly higher than in RCP2.6. For example, only about one-fifth (21%) of weak El Niños can break the GMST record in RCP2.6. The chance significantly

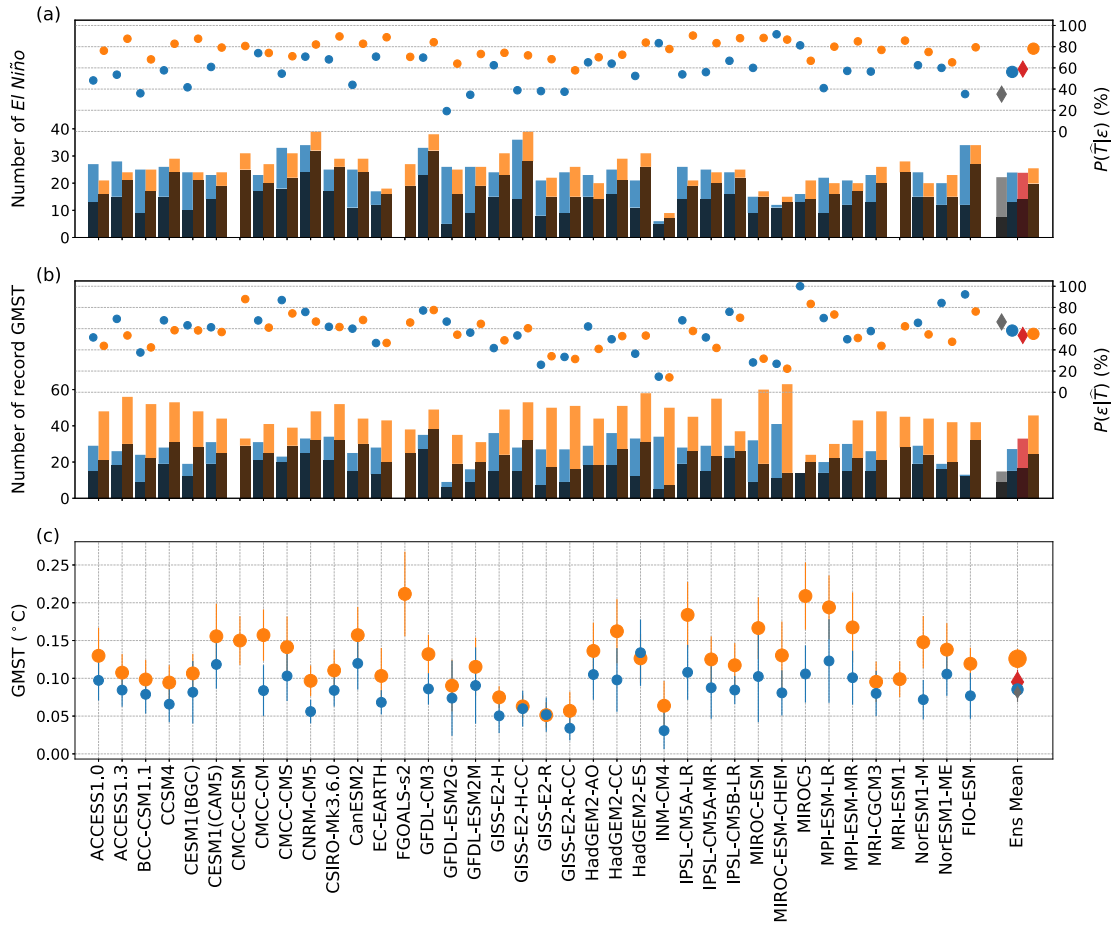

Figure 3. (a) The total numbers of El Niño events during 2006–2100 (N_ϵ) are shown as colored bars for RCP4.5 (blue), RCP8.5 (orange), RCP2.6 (gray), and RCP6.0 (red). The black shaded bars show the numbers of El Niños that cause record-breaking annual GMSTs ($N_\epsilon(\widehat{T} \cap \epsilon)$). The likelihoods of an El Niño to break the GMST record ($P(\widehat{T}|\epsilon)$) are shown in dots (RCP4.5 and RCP8.5) and diamonds (RCP2.6 and RCP6.0) with colors corresponding to different RCPs. (b) The total numbers of record-breaking GMSTs ($N_{\widehat{T}}$) are shown as colored bars (same as (a), representing different RCPs). The black shaded bars show the numbers of record-breaking GMSTs caused by El Niños ($N_{\widehat{T}}(\widehat{T} \cap \epsilon)$). The likelihoods of an record-breaking annual GMST associated with an El Niño ($P(\epsilon|\widehat{T})$) are shown in colored dots and diamonds (same as (a), representing different RCPs). (c) The record-breaking magnitudes of annual GMSTs caused by El Niños ($M(\widehat{T}|\epsilon)$) are shown as colored dots and diamonds (same as (a), representing different RCPs). The error bars represent the 95% confidence intervals of the means. The multi-model ensemble means are shown in the far right of each panel. Individual model results with all four RCPs can be viewed in figure S5.

Table 1. CMIP5 ensemble mean values under different RCPs and El Niño strength.

Variable (unit)	El Niño strength	RCP2.6	RCP4.5	RCP6.0	RCP8.5
$P(\widehat{T}\|\epsilon)$ (%)	ONI $>$ 0.5 (all)	35 ± 5	56 ± 5	59 ± 5	78 ± 3
	0.5 $<$ ONI $\leqslant$ 1.0 (weak)	21 ± 7	37 ± 8	36 ± 12	68 ± 8
	1.0 $<$ ONI $\leqslant$ 1.5 (moderate)	36 ± 11	55 ± 9	54 ± 15	70 ± 8
	ONI $>$ 1.5 (strong)	53 ± 14	78 ± 7	83 ± 8	86 ± 8
$P(\epsilon\|\widehat{T})$ (%)	ONI $>$ 0.5 (all)	66 ± 10	58 ± 7	54 ± 10	55 ± 5
	0.5 $<$ ONI $\leqslant$ 1.0 (weak)	11 ± 4	13 ± 3	10 ± 3	11 ± 2
	1.0 $<$ ONI $\leqslant$ 1.5 (moderate)	20 ± 6	19 ± 4	19 ± 7	16 ± 3
	ONI $>$ 1.5 (strong)	35 ± 11	27 ± 8	25 ± 12	28 ± 7
$M(\widehat{T}\|\epsilon)$ (°C)	ONI $>$ 0.5 (all)	0.08 ± 0.01	0.09 ± 0.01	0.10 ± 0.02	0.13 ± 0.01
	0.5 $<$ ONI $\leqslant$ 1.0 (weak)	0.05 ± 0.01	0.06 ± 0.01	0.07 ± 0.02	0.09 ± 0.01
	1.0 $<$ ONI $\leqslant$ 1.5 (moderate)	0.07 ± 0.01	0.09 ± 0.01	0.10 ± 0.03	0.11 ± 0.01
	ONI $>$ 1.5 (strong)	0.09 ± 0.02	0.10 ± 0.01	0.11 ± 0.03	0.16 ± 0.02

Note. $P(\widehat{T}|\epsilon)$ represents, in all El Niño events, the probability of an El Niño to induce a record-breaking GMST. $P(\epsilon|\widehat{T})$ represents, in all record-breaking GMSTs, the probability of those induced by an El Niño. $M(\widehat{T}|\epsilon)$ represents the average magnitude of a record-breaking GMST associated with El Niño. Error bar represents 95% confidence interval.

increases to two-thirds (68%) in RCP8.5. The result implies that the increase of emissions from RCP2.6 to RCP8.5 significantly increases $P(\widehat{T}|\epsilon)$ regardless of the strength of El Niño. Strong El Niños in the high emission scenarios (RCP8.5) are very likely (86%) to break the GMST record.

Between RCP8.5 and RCP4.5, in which we have the most available models, we find that only the weak and moderate El Niño cases show statistical significance in the differences of $P(\widehat{T}|\epsilon)$. The differences between RCP4.5 and RCP8.5 in $P(\widehat{T}|\epsilon)$ decrease when El Niño strength increases, from 31 ± 11% (weak El Niño) and 16 ± 12% (moderate El Niño) to 8 ± 10% (strong El Niño). The error bar of $P(\widehat{T}|\epsilon)$ difference does not change much between categories, but the difference in the strong case is around 75% smaller than in the weak case. This relatively small difference between RCP4.5 and RCP8.5 in the strong El Niño case implies a 'saturation' of $P(\widehat{T}|\epsilon)$. In other words, strong El Niño can trigger a GMST variation large enough to ensure a record-breaking year regardless of the differences in warming rates between the two scenarios.

3.2. Record-breaking magnitude of GMST during El Niño

Figure 3(c) shows the average record-breaking magnitude of GMST during El Niño ($M(\widehat{T}|\epsilon)$) by considering all El Niños. The $M(\widehat{T}|\epsilon)$ values range from 0.03 ± 0.02 °C to 0.21 ± 0.04 °C. For most models, $M(\widehat{T}|\epsilon)$ is higher under a higher emission scenario. The ensemble mean of $M(\widehat{T}|\epsilon)$ in RCP8.5 shows a record-breaking magnitude of 0.13 ± 0.01 °C and its differences with other RCPs are all statistically significant (table 1). To highlight the important role of El Niño in record-breaking GMSTs, we apply the bootstrapping method with 1000 iterations in each RCP scenario and compare the average magnitudes of record-breaking GMSTs during El Niños and during non El Niños. In all RCPs, the average magnitudes are larger during El Niños than during non El Niños. We find differences of 0.06 ± 0.01 °C in RCP8.5, 0.05 ± 0.01 °C in RCP6.0, 0.04 ± 0.01 °C in RCP4.5, and 0.04 ± 0.01 °C in RCP2.6.

By considering different El Niño strengths, $M(\widehat{T}|\epsilon)$ also shows a higher value under higher emission scenarios (table 1). Despite the differences in $M(\widehat{T}|\epsilon)$ between RCP2.6, RCP4.5, and RCP6.0 not being statistically significant under the same El Niño category, the differences between RCP8.5 and RCP4.5/RCP2.6 appear to be statistically significant regardless of the El Niño category. This shows that $M(\widehat{T}|\epsilon)$ is critically influenced by external forcing. By reducing emissions, we can reduce the average magnitude of a record-breaking GMST during El Niño. However, one should be aware that reducing emissions also decreases the total numbers of record-breaking GMSTs (figure 3(b)). In addition, a stronger El Niño also shows higher $M(\widehat{T}|\epsilon)$ under fixed RCP, which is expected due to a larger GMST variation that can be induced by a stronger El Niño. The differences in $M(\widehat{T}|\epsilon)$ between weak and strong El Niños show statistical significance in all RCPs.

3.3. Likelihood of record-breaking GMST linked to an El Niño during the 21st century

Since El Niño is not the only factor to cause a record-breaking GMST, we calculate the likelihood for a record-breaking GMST being associated with an El Niño event ($P(\epsilon|\widehat{T})$). The total number of record-breaking GMSTs ($N_{\widehat{T}}$) is closely correlated with the strength of emissions in all models (figure 3(b)). The positive correlation between the emission scenario and the number of record-breaking GMSTs associated with El Niño ($N_{\widehat{T}}(\widehat{T} \cap \epsilon)$) is also evident in most models. Interestingly, figure 3(b) and table 1 show a decreasing $P(\epsilon|\widehat{T})$ when emission increases, which is opposite to $P(\widehat{T}|\epsilon)$.

$P(\epsilon|\widehat{T})$ in RCP2.6 is higher than all other RCPs (table 1). In other words, the result suggests that there are higher chances for a record-breaking GMST to be associated with El Niño in a low emission scenario than in high emission scenario. However, due to the large uncertainty and relatively small difference in $P(\epsilon|\widehat{T})$, we find no statistical significance in the difference between RCPs. In all RCPs, more than half of the record-breaking GMSTs are associated with an El Niño. In the piControl run, on the other hand, the ONI changes can explain a little more than one-quarter of the GMST variance with a three-month lag, which is consistent with the result in Trenberth (2002). These results confirm that, among various factors, El Niño is perhaps most dominant in causing record-breaking GMSTs on interannual timescale. Therefore, when the warming trend in GMST due to RCP forcing is small, other factors that generate smaller GMST variations than El Niño are 'over-shadowed' by the GMST records induced by El Niños. This is consistent with the bootstrapping test which shows the average magnitudes of record-breaking GMSTs are larger during El Niños than during non El Niños. Under moderate and strong El Niño cases, we see the same phenomenon of high $P(\epsilon|\widehat{T})$ in a low emission scenario. We also see that, in all RCPs, more record-breaking GMSTs are generated by strong El Niños than weaker El Niños.

3.4. Influence of different types of El Niño

Many studies have shown that the two types of El Niño, central Pacific El Niño (CP) and eastern Pacific El Niño (EP), are related to different mechanisms and teleconnections (e.g. Larkin and Harrison 2005, Ashok *et al* 2007, Kao and Yu 2009). CP and EP El Niños differ in their location of SST maximum in the tropical Pacific. By following Yu and Kim (2013), we classify the El Niño events to CP and EP. There are more CPs

Table 2. CMIP5 ensemble mean values under different RCPs and El Niño types.

Variable (unit)	El Niño type	RCP2.6	RCP4.5	RCP6.0	RCP8.5
$P(\widehat{T}\|\epsilon)$ (%)	CP	29 ± 7	49 ± 6	50 ± 8	76 ± 4
	EP	42 ± 10	58 ± 8	61 ± 11	74 ± 5
$P(\epsilon\|\widehat{T})$ (%)	CP	33 ± 8	29 ± 6	25 ± 8	30 ± 5
	EP	29 ± 9	25 ± 6	22 ± 8	23 ± 4
$M(\widehat{T}\|\epsilon)$ (°C)	CP	0.08 ± 0.01	0.08 ± 0.01	0.07 ± 0.02	0.12 ± 0.01
	EP	0.07 ± 0.02	0.08 ± 0.01	0.10 ± 0.02	0.13 ± 0.01

Note. $P(\widehat{T}|\epsilon)$ represents, in all El Niño events, the probability of an El Niño to induce record-breaking GMST. $P(\epsilon|\widehat{T})$ represents, in all record-breaking GMSTs, the probability of those induced by an El Niño. $M(\widehat{T}|\epsilon)$ represents the average magnitude of record-breaking GMST associated with El Niño. Error bar represents 95% confidence interval.

than EPs in all RCP scenarios (table 2, figures S9–S10), which is in consistent with Kim and Yu (2012). As a result, the larger $P(\epsilon|\widehat{T})$ in CP compared to EP shows that there are more CP-related record-breaking GMSTs than EP-related. However, the differences are not large enough to be statistically significant. On the other hand, EP shows larger $P(\widehat{T}|\epsilon)$ than CP in all RCPs except RCP8.5, which means that a record-breaking GMST is more likely to happen once EP occurs. This could relate to the increasing occurrence of strong EP events under a warming climate (Cai *et al* 2018), which makes EP more likely to generate a record-breaking GMST than CP. However, the differences in $P(\widehat{T}|\epsilon)$ are not large enough to show statistical significance, either. The two types of El Niño generate similar $M(\widehat{T}|\epsilon)$ under different RCP scenarios. The above analyses suggest a more dominant role of RCP scenarios over types of El Niño in all statistics.

Since the discovery of different types of El Niño, new classifications have been proposed to better capture different SST spatial patterns (e.g. Ren and Jin 2011, Kim and Yu 2012). Considering the large number of CMIP models used here and their different simulations for El Niño, we choose a relatively simple and straightforward classification method based on ONI. Nonetheless, it is not perfect, as the ONI is based on a fixed location over the ocean. If future El Niños evolve to a different spatial pattern, the statistics might be affected.

3.5. Inter-comparison between CMIPs

To verify if the results are affected by the development and improvement of the climate models, we conduct the same analyses for the CMIP3 and the available CMIP6 models so far on the Earth System Grid Federation (ESGF) database (downloaded as of 6/3/2019). As a common experiment across CMIPs, we use the 1% per year CO_2 increase (1pctCO_2) experiment to complete the inter-comparison of different phases of CMIP (figure S11–S13). We choose the first 80 years in the 1pctCO_2 experiments. The ensemble mean of $P(\widehat{T}|\epsilon)$ in CMIP3 is 64 ± 8% compared to 70 ± 4% in CMIP5 and 69 ± 6% in CMIP6 (figure 4(a)). All ensemble means are reasonably close with a maximum difference of 6 ± 9% in $P(\widehat{T}|\epsilon)$. CMIP3 shows a larger spread in $P(\widehat{T}|\epsilon)$ between models when compared to CMIP5 and CMIP6. This might be related to the model convergence in simulating El Niño-Southern oscillation (ENSO) frequency and amplitude as pointed out in the Intergovernmental Panel on Climate Change (IPCC) Fifth Assessment Report (Flato *et al* 2013). The ensemble mean of $M(\widehat{T}|\epsilon)$ in CMIP3 is 0.11 ± 0.01 °C compared to 0.10 ± 0.01 °C in CMIP5 and 0.12 ± 0.02 °C in CMIP6 (figure 4(c)) with a maximum difference of 0.02 ± 0.03 °C. We see similar standard deviation of $M(\widehat{T}|\epsilon)$ in all CMIPs. Finally, the ensemble means of $P(\epsilon|\widehat{T})$ show a value of 64 ± 11% in CMIP3 compared to 55 ± 6% in CMIP5 and 73 ± 13% in CMIP6 (figure 4(b)). The larger uncertainty and higher value in CMIP6 when compared to other CMIPs are largely due to the small number of available models (nine CMIP6 models thus far) and two relatively high $P(\epsilon|\widehat{T})$ values from the Goddard Institute for Space Studies center. Therefore, the question of whether there is an increase in record-breaking GMST caused by El Niño in CMIP6 still needs further investigation. For $P(\epsilon|\widehat{T})$, CMIP3 still shows the largest variability between models with standard deviation of 22% compared to 14% in CMIP5 and 17% in CMIP6.

3.6. Comparison between model result and observation

The nature of the CMIP5 design is such that the model simulations do not attempt to capture individual events as in the observation, but rather to obtain the long-term statistics. A short-term mean would be susceptible to a specific event during the averaging period (i.e. timing and response of the event). For instance, considering an El Niño cycle of five years during a 30-year period, the count for just one El Niño could cause ~17% difference in $P(\widehat{T}|\epsilon)$. A long-term mean with a larger sample size of El Niño would make the statistics more robust. However, the observed record-breaking GMSTs associated with an El Niño event only become less uncertain after 1980 due to

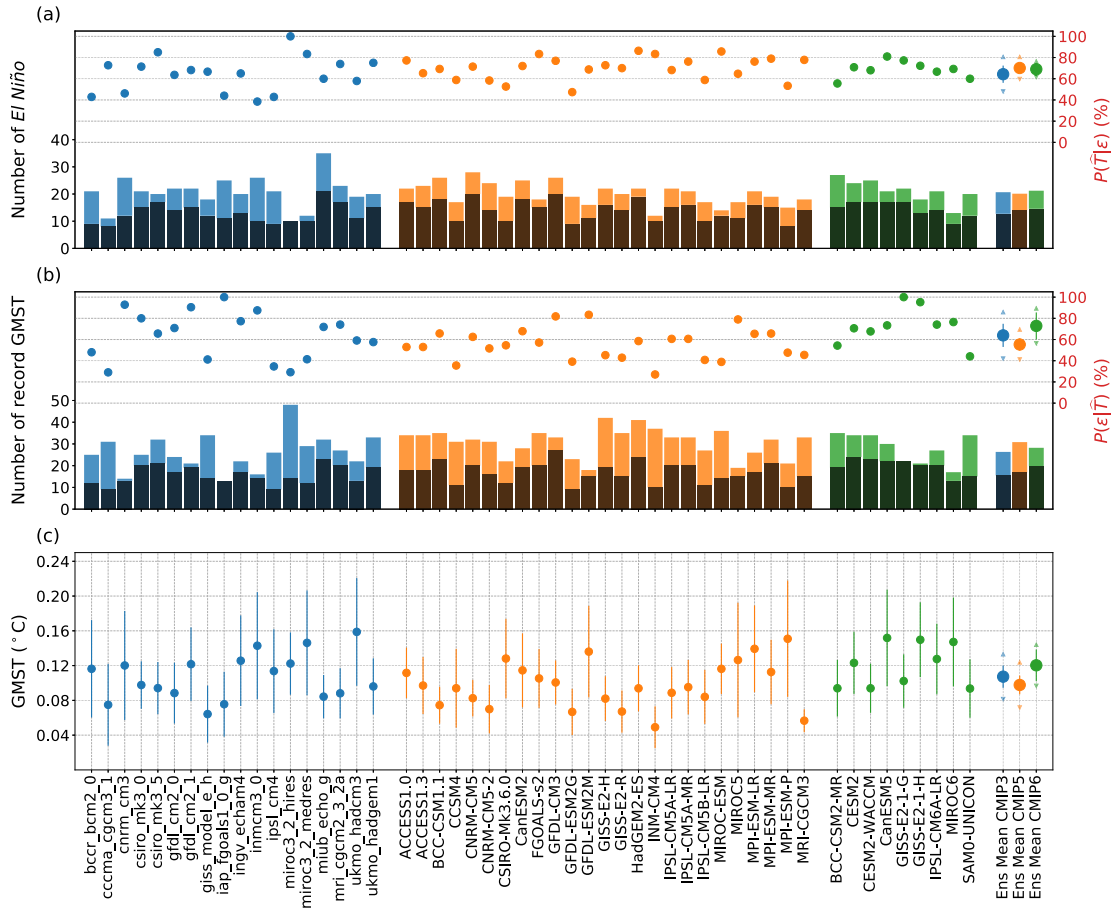

Figure 4. (a) The total numbers of El Niños (N_ϵ) are shown as colored bars for CMIP3 models (blue), CMIP5 models (orange), and CMIP6 models (green). The black shaded bars show the numbers of El Niños associated with record-breaking annual GMSTs ($N_\epsilon(\widehat{T} \cap \epsilon)$). The likelihoods of record-breaking annual GMSTs during El Niños ($P(\widehat{T}|\epsilon)$) are shown in dots with the color corresponding to the different CMIPs. (b) The total numbers of record-breaking GMSTs ($N_{\widehat{T}}$) are shown as colored bars (same as (a), representing different CMIPs). The black shaded bars show the numbers of record-breaking GMSTs associated with El Niños ($N_{\widehat{T}}(\widehat{T} \cap \epsilon)$). The likelihoods of record-breaking annual GMSTs associated with El Niños ($P(\epsilon|\widehat{T})$) are shown in dots with the color corresponding to different CMIPs. (c) The magnitudes of record-breaking annual GMSTs associated with El Niños ($M(\widehat{T}|\epsilon)$) are shown in dots with the colors corresponding to different CMIPs (same as (a)). The error bars represent the 95% confidence intervals of the means. The multi-model ensemble means are shown in the far right of each panel with error bars (95% confidence interval) and standard deviation ranges (upward and downward triangles).

improvement of data spatial coverage (Cowtan *et al* 2018), and are less affected by volcanic activities.

Due to the reasons above, we focus the comparison on $M(\widehat{T}|\epsilon)$ between models and observations. Yin *et al* (2018) show observed record-breaking magnitude ranging from 0.02 °C to 0.24 °C and a value of 0.08 °C in $M(\widehat{T}|\epsilon)$ during 1980–2016. This observed $M(\widehat{T}|\epsilon)$ agrees well with the value of 0.08 ± 0.01 °C in the CMIP5 historical run. A regression between GMST and ONI which shows 0.09 ± 0.02 °C per ONI in the piControl run also agrees well with 0.08 °C per Nino3.4 index based on observations (Trenberth 2002). The two particularly large record-breaking GMSTs (0.19 °C during 1997–98 El Niño and 0.24 °C during 2015-16 El Niño) are also within the range of $M(\widehat{T}|\epsilon)$ estimates in CMIP5 models (0.03 ± 0.02 °C to 0.21 ± 0.04 °C).

We further calculate the difference between historical simulation and future projections (RCPs), and find that the differences in $M(\widehat{T}|\epsilon)$ show no statistical significance in all RCPs except in RCP8.5, which shows a difference of 0.05 ± 0.01 °C and increases in magnitude. Historical simulation shows 25 ± 3% in $P(\widehat{T}|\epsilon)$ and 65 ± 6% in $P(\epsilon|\widehat{T})$. For $P(\widehat{T}|\epsilon)$, all RCPs (table 1) are larger than the historical simulation with differences showing statistical significance. For $P(\epsilon|\widehat{T})$, only RCP8.5 shows a difference of 10 ± 8% and is smaller than the historical simulation.

While the models have global coverage, some observational datasets (e.g., HadCRUT4 (Morice *et al* 2012)) do not. To investigate if the spatial coverage affects the statistics in this study, we apply the HadCRUT4 mask to the model output. The GMST from the masked model output only shows a variance change of 0.1% which includes the trend difference mainly due to the difference in polar region coverage. The comparison shows few changes in magnitude (<0.01 °C) and less than 3% changes in both $P(\widehat{T}|\epsilon)$ and $P(\epsilon|\widehat{T})$ except for a 6% decreases in $P(\epsilon|\widehat{T})$ for RCP2.6. All differences between masked and

unmasked estimates are within the error bar provided in this study.

4. Conclusions

In this study, we investigate the combination of the strong and transient warmth induced by El Niño with the gradual and persistent warming induced by greenhouse gas forcing (figure 2). We focus on the multi-model ensemble statistics of record-breaking global mean surface temperature (GMST) induced by El Niño. These statistics include both frequency and magnitude from CMIP5 projections for the 21st century. The emission scenario has a significant influence on the likelihood of record-breaking GMST happening during El Niño ($P(\widehat{T}|\epsilon)$), with stronger emission scenarios causing higher $P(\widehat{T}|\epsilon)$. Under a low emission scenario (RCP2.6), one out of three El Niño events breaks the GMST record during the 21st century. The probability increases to four out of five in a high emission scenario (RCP8.5). The result shows the importance of climate change mitigation in reducing record-breaking GMSTs during important internal variability such as El Niño. However, the emission scenario has a limited influence on the likelihood of a record-breaking GMST occurring during strong El Niño. A strong El Niño produces a GMST variation that is large enough to break the GMST record regardless of the GMST trend difference between RCP4.5 and RCP8.5. Stronger El Niño also induces a higher record-breaking magnitude ($M(\widehat{T}|\epsilon)$) in each RCP. $M(\widehat{T}|\epsilon)$ can range from 0.03 °C to 0.21 °C based on individual CMIP5 models. El Niño accounts for more than half of record-breaking GMST occurrences in all RCPs. The critical influence of background warming on the statistics of the record-breaking GMST suggests that these statistics could be used to infer or confirm the background warming.

For the likelihood of a record-breaking GMST happening during El Niño and a record-breaking magnitude, the inter-comparison of CMIPs shows a consistent result with little differences. The likelihood for a record-breaking GMST associated with an El Niño ($P(\epsilon|\widehat{T})$) shows little difference between CMIP3 and CMIP5. It should be noted that the statistics in this study are the average for the 21st century. The exact number can change decade by decade due to the nonlinear warming trends such as in RCP2.6 and RCP8.5. For example, in RCP2.6, there is minimal record-breaking GMSTs in the second half of the century due to the deceleration of the warming trend (figure 2). Due to less record-breaking GMSTs associated with El Niño over a shorter period or a result of the nonlinear trend, the resulting larger error bar leads to a less conclusive result from the same analyses. The possible under-represented inter-basin connection and decadal variability in the models could also slightly alter the statistics shown in this study. The inter-basin differences in SST, which are important to the observed low-level easterly wind anomaly over the tropical Pacific, can affect the estimates of long-term Walker circulation change (Zhang and Karnauskas 2016). The under-represented decadal variability, such as Pacific decadal variability, might also affect the simulated El Niño events (Deser *et al* 2011). Another source of uncertainty relating to the statistics would come from possible future volcanic eruptions. Its effect can be seen in the observational data and the historical run. However, where and when future volcanic eruptions will occur in the 21st century is highly uncertain. As such, the IPCC assessments did not incorporate volcanic forcing in the 21st century projections (Pachauri and Meyer 2014). For the same reason, the statistics in this study only focus on the influence of El Niño without considering the volcanic forcing.

Acknowledgments

This study is supported by the NOAA Climate Program Office (grant NA18OAR4310267). We thank Dr Stephen M Griffies and Dr John Krasting at NOAA/GFDL for the helpful comments on the manuscript. The authors thank the editor and the anonymous reviewers for their advice on improving this manuscript. We thank the CMIP group and modeling centers for providing the simulated data (tables S1–S3) and also the data hosting center at the Earth System Grid Federation (ESGF). The simulated data used in the study are available from the Earth System Grid (https://esgf.llnl.gov).

Data availability statement

The CMIP datasets used in the study are available at the Earth System Grid Federation (ESGF) Peer-to-Peer (P2P) enterprise system (https://esgf-node.llnl.gov/projects/esgf-llnl/). The statistical results derived from the datasets that support the findings of this study are openly available (https://bit.ly/2MPtS2i). The code to reproduce the results in the study from CMIP datasets are openly available at this GitHub repository (https://github.com/chiaweh2/ElNino_record_GMST).

ORCID iDs

Chia-Wei Hsu https://orcid.org/0000-0002-4838-0140

References

Ashok K, Behera S K, Rao S A, Weng H and Yamagata T 2007 El Niño Modoki and its possible teleconnection *J. Geophys. Res. Oceans* **112** C11007

Bellenger H, Guilyardi E, Leloup J, Lengaigne M and Vialard J 2014 ENSO representation in climate models: From CMIP3 to CMIP5 *Clim. Dyn.* **42** 1999–2018

Buermann W, Anderson B, Tucker C J, Dickinson R E, Lucht W, Potter C S and Myneni R B 2003 Interannual covariability in Northern Hemisphere air temperatures and greenness associated with El Niño-Southern Oscillation and the Arctic Oscillation *J. Geophys. Res. Atmos.* **108** 4396

Cai W, Wang G, Dewitte B, Wu L, Santoso A, Takahashi K, Yang Y, Carréric A and McPhaden M J 2018 Increased variability of eastern Pacific El Niño under greenhouse warming *Nature* **564** 201

Chen C, Cane M A, Wittenberg A T and Chen D 2016 ENSO in the CMIP5 simulations: life cycles, diversity, and responses to climate change *J. Clim.* **30** 775–801

Cowtan K, Jacobs P, Thorne P and Wilkinson R 2018 Statistical analysis of coverage error in simple global temperature estimators *Dyn. Stat. Clim. Syst.* **3** dzy003

Deser C, Phillips A S, Tomas R A, Okumura Y M, Alexander M A, Capotondi A, Scott J D, Kwon Y-O and Ohba M 2011 ENSO and pacific decadal variability in the community climate system model version 4 *J. Clim.* **25** 2622–51

Flato G *et al* 2013 Evaluation of climate models *Climate Change 2013: The Physical Science Basis. Contribution of Working Group I to the Fifth Assessment Report of the Intergovernmental Panel on Climate Change* ed T F Stocker *et al* (Cambridge: Cambridge University Press) pp 741–866

Foster G and Rahmstorf S 2011 Global temperature evolution 1979-2010 *Environ. Res. Lett.* **6** 044022

Kao H-Y and Yu J-Y 2009 Contrasting Eastern-Pacific and Central-Pacific Types of ENSO *J. Clim.* **22** 615–32

Kim S T and Yu J-Y 2012 The two types of ENSO in CMIP5 models *Geophys. Res. Lett.* **39** L11704

Larkin N K and Harrison D E 2005 On the definition of El Niño and associated seasonal average US weather anomalies *Geophys. Res. Lett.* **32** L13705

Meehl G A, Hu A, Santer B D and Xie S-P 2016 Contribution of the Interdecadal Pacific Oscillation to twentieth-century global surface temperature trends *Nat. Clim. Change* **6** 1005–8

Morice C P, Kennedy J J, Rayner N A and Jones P D 2012 Quantifying uncertainties in global and regional temperature change using an ensemble of observational estimates: the HadCRUT4 data set *J. Geophys. Res. Atmos.* **117** D08101

Muller R A, Curry J, Groom D, Jacobsen R, Perlmutter S, Rohde R, Rosenfeld A, Wickham C and Wurtele J 2013 Decadal variations in the global atmospheric land temperatures *J. Geophys. Res. Atmospheres* **118** 5280–6

Newell R E and Weare B C 1976 Factors governing tropospheric mean temperature *Science* **194** 1413–4

Pachauri R K and Meyer L A (ed) 2014 *Climate Change 2014: Synthesis Report. Contribution of Working Groups I, II and III to the Fifth Assessment Report of the Intergovernmental Panel on Climate Change* (Geneva: IPCC) 151 pp (https://www.ipcc.ch/report/ar5/syr/)

Palmer T, Doblas-Reyes F, Hagedorn R and Weisheimer A 2005 Probabilistic prediction of climate using multi-model ensembles: from basics to applications *Philos. Trans. R. Soc. Lond. B. Biol. Sci.* **360** 1991–8

Pan Y H and Oort A H 1983 Global climate variations connected with sea surface temperature anomalies in the eastern equatorial pacific ocean for the 1958-73 Period *Mon. Wea. Rev.* **111** 1244–58

Power S B and Delage F P D 2019 Setting and smashing extreme temperature records over the coming century *Nat. Clim. Change* **9** 529

Ren H-L and Jin F-F 2011 Niño indices for two types of ENSO *Geophys. Res. Lett.* **38** L04704

Schlesinger M E and Ramankutty N 1994 An oscillation in the global climate system of period 65-70 years *Nature* **367** 723

Schleussner C F, Runge J, Lehmann J and Levermann A 2014 The role of the North Atlantic overturning and deep ocean for multi-decadal global-mean-temperature variability *Earth Syst. Dyn.* **5** 103–15

Su J, Zhang R and Wang H 2017 Consecutive record-breaking high temperatures marked the handover from hiatus to accelerated warming *Sci. Rep.* **7** 43735

Taylor K E, Stouffer R J and Meehl G A 2011 An Overview of CMIP5 and the experiment design *Bull. Amer. Meteor. Soc.* **93** 485–98

Tebaldi C and Knutti R 2007 The use of the multi-model ensemble in probabilistic climate projections *Philos. Trans. R. Soc. Lond. A. Math. Phys. Engi. Sci.* **365** 2053–75

Timmermann A, Oberhuber J, Bacher A, Esch M, Latif M and Roeckner E 1999 Increased El Niño frequency in a climate model forced by future greenhouse warming *Nature* **398** 694

Trenberth K 2018 *The Climate Data Guide: Nino SST Indices (Nino 1 +2, 3, 3.4, 4; ONI and TNI)* (https://climatedataguide.ucar.edu/climate-data/nino-sst-indices-nino-12-3-34-4-oni-and-tni)

Trenberth K E 2002 Evolution of El Niño–Southern Oscillation and global atmospheric surface temperatures *J. Geophys. Res.* **107** 4065

Wergen G and Krug J 2010 Record-breaking temperatures reveal a warming climate *EPL Europhys. Lett.* **92** 30008

Wittenberg A T, Rosati A, Delworth T L, Vecchi G A and Zeng F 2014 ENSO Modulation: is it decadally predictable? *J. Clim.* **27** 2667–81

Yin J, Overpeck J, Peyser C and Stouffer R 2018 Big jump of record warm global mean surface temperature in 2014-2016 related to unusually large oceanic heat releases *Geophys. Res. Lett.* **45** 1069–78

Yu J-Y and Kim S T 2013 Identifying the types of major El Niño events since 1870 *Int. J. Climatol.* **33** 2105–12

Zanchettin D, Bothe O, Graf H F, Lorenz S J, Luterbacher J, Timmreck C and Jungclaus J H 2013 Background conditions influence the decadal climate response to strong volcanic eruptions *J. Geophys. Res. Atmospheres* **118** 4090–106

Zhang L and Karnauskas K B 2016 The role of tropical interbasin sst gradients in forcing walker circulation trends *J. Clim.* **30** 499–508

Zhang R, Delworth T L and Held I M 2007 Can the Atlantic Ocean drive the observed multidecadal variability in Northern Hemisphere mean temperature? *Geophys. Res. Lett.* **34** L02709